

Multi-Task Learning for Metal Alloy Property Prediction: An Empirical Study of Negative Transfer and Mitigation Strategies

Sungwoo Kang^a,

^a*Department of Electrical and Computer Engineering, Korea University, Seoul 02841, Republic of Korea*

Abstract

Multi-task learning (MTL) in materials science rests on a fundamental assumption: that physically related properties—such as electrical resistivity and mechanical hardness, which both depend on atomic-level factors—share mathematical representations suitable for joint learning. We challenge this assumption through a systematic investigation using the AI-Hub Korea metal alloy dataset (54,028 samples), which exhibits extreme task-level data imbalance (65:1) representative of real-world materials databases where some properties are far easier to measure than others.

Our results reveal a striking dichotomy: MTL *significantly degrades* regression performance (resistivity R^2 : 0.897 \rightarrow 0.844, $p < 0.01$; hardness R^2 : 0.832 \rightarrow 0.694, $p < 0.01$) while *significantly improving* classification performance (amorphous-forming ability recall improved by 17%, $p < 0.05$). We trace this divergence to a fundamental mismatch in functional forms: resistivity follows element-wise polynomial dependence (Nordheim rule, $R^2 = 0.74$), while hardness exhibits different compositional dependencies, creating gradient directions misaligned by 66–75° during optimization. Learned task relation graphs confirm this incompatibility, revealing near-zero inter-task weights (~ 0.006).

Evaluating Deep Imbalanced Regression mitigation techniques, we find that projecting conflicting gradient components (PCGrad) recovers and surpasses single-task performance for hardness ($R^2 = 0.855$, +12.4%), while LDS+GradNorm achieves the best overall balance across all tasks. These findings yield an actionable framework: use independent models for high-precision material characterization, but consider MTL for high-throughput screening where improved recall reduces missed discoveries. We propose a “materials property clustering” hypothesis—that properties sharing physical mechanisms (electronic, mechanical, thermodynamic) may benefit from joint learning, while cross-mechanism MTL requires explicit validation—though we emphasize that this case study on the AI-Hub dataset requires replication on independent experimental databases before general principles can be established.

Keywords: multi-task learning, negative transfer, metal alloys, property prediction, machine learning, materials informatics

Email address: krm1919@korea.ac.kr (Sungwoo Kang)

1. Introduction

The accelerated discovery of advanced materials with tailored properties is a central goal of modern materials science. Machine learning (ML) has emerged as a powerful tool in this endeavor, enabling rapid prediction of material properties from composition and structure descriptors [1, 2]. Among ML approaches, multi-task learning (MTL) has garnered significant attention for its promise to improve prediction accuracy by jointly learning multiple related properties [3].

The appeal of MTL in materials science rests on a fundamental assumption: that different material properties share underlying physical mechanisms, and thus learning to predict one property can provide useful inductive bias for predicting others [3]. For metal alloys, this assumption appears intuitive—electrical resistivity, mechanical hardness, and glass-forming ability are all influenced by atomic-level factors such as electronegativity differences, atomic size mismatch, and mixing enthalpy [4]. This has motivated numerous studies applying transfer learning [5, 6] and multi-task learning [7] to materials property prediction.

However, this reasoning conflates two distinct concepts: *physical relatedness* and *statistical transferability*. While resistivity and hardness may both depend on atomic descriptors, they follow fundamentally different functional forms—element-wise polynomial dependence (Nordheim rule) versus power-law lattice distortion dependence. A neural network backbone cannot simultaneously be an optimal polynomial estimator and an optimal power-law estimator. Blindly applying MTL without considering these structural differences risks negative transfer, where the dominant task’s functional bias corrupts learning for other tasks.

The machine learning community has documented this phenomenon extensively [8, 9], yet it has received insufficient attention in materials informatics. This is particularly concerning when datasets are severely imbalanced across tasks, as the optimization may be dominated by the largest task at the expense of smaller ones [10]. We deliberately investigate such a “real-world” scenario: the AI-Hub Korea metal alloy dataset exhibits extreme data imbalance (65:1 ratio between resistivity and hardness samples), a common yet understudied condition in materials databases where some properties are far easier to measure than others.

This work addresses three research questions that challenge common assumptions in materials informatics:

- **RQ1 (The Myth):** Does physical relatedness between material properties guarantee positive transfer in multi-task learning, or do functional form mismatches create interference?
- **RQ2 (The Stress Test):** How does extreme, real-world data imbalance (e.g., 65:1) impact the optimization dynamics of shared representations compared to independent learning?
- **RQ3 (The Utility):** In the presence of negative transfer for regression, can MTL still provide practical utility for material screening and candidate discovery?

To answer these questions, we make the following contributions:

1. We construct a comprehensive benchmark using the AI-Hub Korea metal alloy dataset, containing 54,028 unique samples with three target properties: electrical resistivity (52,388 samples), Vickers hardness (800 samples), and amorphous-forming ability (840 samples).
2. We implement and compare three modeling approaches: independent single-task neural networks, standard MTL with hard parameter sharing, and structured MTL with learned task relation graphs.
3. We identify a fundamental trade-off in MTL utility for materials science: while shared representations degrade high-precision property regression due to gradient conflicts (resistivity R^2 : -5.9% ; hardness R^2 : -16.6%), they significantly improve candidate screening capabilities for classification tasks (recall $+17\%$). This yields an actionable guideline: use independent models for material characterization (where precision matters), but consider MTL for high-throughput discovery pipelines (where recall matters).
4. We trace the root causes of negative transfer to functional form mismatch (gradient angles of $66\text{--}75^\circ$) and task-level data imbalance, with learned task relations confirming property independence (inter-task weights ~ 0.006).
5. We evaluate Deep Imbalanced Regression mitigation techniques, demonstrating that PCGrad recovers $+12.4\%$ on the minority task while LDS+GradNorm achieves the best overall balance—providing practitioners with validated tools for handling imbalanced multi-property datasets.

The remainder of this paper is organized as follows. Section 2 reviews related work on MTL in materials science and the phenomenon of negative transfer. Section 3 describes our dataset, model architectures, and experimental setup. Section 4 presents comprehensive results with statistical analysis. Section 5 analyzes why MTL fails for regression but succeeds for classification, and provides practical recommendations. Section 6 summarizes our findings and outlines future directions.

2. Related Work

2.1. Multi-Task Learning in Materials Science

Multi-task learning has been increasingly applied to materials property prediction, motivated by the hypothesis that related properties share underlying physical principles. Xie and Grossman [5] demonstrated that graph neural networks can learn transferable representations for inorganic crystals, showing that pretraining on formation energy improves band gap prediction. Chen et al. [6] developed AtomSets, a hierarchical transfer learning framework that leverages pre-trained representations on large datasets to improve predictions on smaller target datasets.

For molecular property prediction, Ramsundar et al. [11] showed that MTL on hundreds of biological assays can improve prediction of drug-target interactions. More recently, Wen et al. [12] extended this to reaction property prediction, demonstrating benefits when tasks share chemical mechanisms.

However, most of these studies focus on scenarios where tasks are inherently related (e.g., multiple biological assays for the same target, or properties governed by similar physics). The question of whether arbitrary material properties benefit from joint learning has been less thoroughly examined.

2.2. Negative Transfer and Task Interference

The machine learning community has extensively studied the phenomenon of negative transfer, where knowledge transfer between tasks degrades rather than improves performance [8]. Standley et al. [9] systematically analyzed task relationships in computer vision and found that many seemingly related tasks exhibit negative transfer when trained jointly.

Several factors contribute to negative transfer:

- **Task dissimilarity:** When optimal representations for different tasks conflict, shared parameters are forced into suboptimal compromises [13].
- **Data imbalance:** When tasks have vastly different sample sizes, gradient updates are dominated by the larger task, starving smaller tasks of learning signal [10].
- **Gradient interference:** Conflicting gradient directions across tasks can cause optimization instabilities [14].

Chen et al. [10] proposed GradNorm to dynamically balance gradient magnitudes across tasks, partially mitigating imbalance effects. Kendall et al. [15] introduced uncertainty-based task weighting. However, these methods address symptoms rather than the fundamental question of task compatibility. A comprehensive survey of negative transfer phenomena is provided by Zhang et al. [16].

2.3. Deep Imbalanced Regression

While class imbalance has been extensively studied in classification, the analogous problem for regression—termed *Deep Imbalanced Regression* (DIR)—has received attention only recently [17]. In DIR, the target variable y is continuous, and the challenge is that certain regions of the target space are underrepresented in training data. This is particularly relevant for materials science, where experimental measurements often cluster around common property values while extreme values are rare.

Yang et al. [17] formalized DIR and proposed two key techniques. First, *Label Distribution Smoothing* (LDS) estimates the effective label density by convolving the empirical distribution with a symmetric kernel:

$$\tilde{p}(y) = \int K(y, y')p(y')dy' \tag{1}$$

where K is typically a Gaussian kernel. This smoothed density enables principled reweighting of samples from underrepresented regions. Second, *Feature Distribution Smoothing* (FDS) applies similar smoothing in feature space to prevent overfitting to majority-region features.

Ren et al. [18] extended this work with *Balanced MSE*, which reformulates the standard MSE loss to account for label imbalance:

$$\mathcal{L}_{BMC} = -\log \mathbb{E}_{y \sim p_{train}(y)} [\mathcal{N}(y|f(x), \sigma^2)] \quad (2)$$

This formulation prevents the model from collapsing predictions toward the mode of the training distribution.

These techniques are directly relevant to MTL scenarios with severely imbalanced task sizes. When one task dominates training (as in our 65:1 resistivity-to-hardness ratio), the shared backbone effectively experiences a form of “task-level” imbalanced regression, where the minority task’s signal is overwhelmed by the majority task’s gradients.

2.4. Task Relation Learning

Rather than assuming task relationships a priori, recent work has explored learning task relations directly from data. Zamir et al. [19] computed a “taskonomy” revealing which visual tasks transfer well to others. For molecular property prediction, several studies have learned task graphs indicating which properties provide useful auxiliary information for others [20].

In materials science, explicit task relation learning remains underexplored. Most MTL studies either assume all properties are related (fully shared representations) or manually specify which properties should be grouped. Our work addresses this gap by learning task relations for metal alloy properties and using the learned structure to understand MTL performance.

2.5. MTL for Metal Alloys

Metal alloys present an interesting case study for MTL due to the complex interplay of their properties. High-entropy alloys (HEAs) in particular have attracted attention for their unusual property combinations [4]. Several studies have applied ML to predict HEA properties:

Debnath et al. [7] used MTL to predict yield strength and elongation of HEAs, finding modest improvements. Pei et al. [21] predicted hardness and phase stability using composition features. More recently, Kamnis et al. [22] demonstrated that transformer-based language models can effectively predict HEA mechanical properties by treating compositions as sequences, achieving strong performance through *sequential* transfer learning (pre-train then fine-tune) rather than simultaneous MTL. Rao et al. [23] showed that active learning approaches, which iteratively select informative samples rather than training on static archives, can discover novel Invar HEAs with high efficiency.

However, most existing studies use small, curated datasets where all samples have all properties labeled—a scenario quite different from the realistic setting where different properties are measured on different sample sets. Furthermore, the question of whether properties from different physical domains (e.g., electronic transport versus mechanical plasticity) can share representations remains largely unexamined.

Our work addresses this realistic scenario using a union dataset approach where each sample may have only a subset of properties labeled, employing masked loss functions to handle missing labels during training. Critically, we examine MTL across physically distinct property types, revealing fundamental limitations of the shared-representation assumption.

2.6. *Contrasting Results in Recent Literature*

Recent studies have reported contrasting results regarding MTL effectiveness for materials property prediction. A 2025 study in *Acta Materialia* demonstrated substantial improvements (+37.5%) using MTL for superalloy property prediction across six thermodynamic and microstructural properties [24]. Similarly, Debnath et al. [7] reported modest improvements when applying MTL to high-entropy alloy (HEA) yield strength and elongation prediction.

These positive results appear to contradict our findings of negative transfer. However, key differences may explain the discrepancy: (1) *Property selection*: The superalloy study predicted properties within the same physical domain (thermodynamic/microstructural), whereas we combine properties from different domains (electronic, mechanical, phase stability); (2) *Data balance*: Different sample size ratios across tasks may determine whether negative transfer occurs; (3) *Material system*: Property relationships may be composition-dependent, with some alloy families exhibiting stronger inter-property correlations than others.

These contrasting results motivate a central question of our study: under what conditions does MTL help versus harm materials property prediction? Rather than assuming universal benefit, we seek to identify factors that determine MTL effectiveness.

3. Methodology

3.1. *Dataset*

We utilize the metal alloy dataset from AI-Hub Korea, which contains experimental measurements of various properties for high-entropy alloys and related metallic systems. The dataset comprises three target properties:

- **Electrical Resistivity** ($\mu\Omega\text{-cm}$): A continuous property measured for 52,388 samples.
- **Vickers Hardness** (GPa): A continuous property measured for 800 samples.
- **Amorphous-Forming Ability**: A binary classification (crystalline/amorphous) with 840 samples.

Critically, these properties were measured on largely non-overlapping sample sets. Traditional MTL approaches require all samples to have all labels, which would yield only a small intersection of samples. Instead, we employ a *union dataset* approach, concatenating all samples and using masked loss functions to handle missing labels. This yields a total of 54,028 samples in the union dataset.

3.1.1. Input Features

Each sample is represented by a 21-dimensional feature vector comprising:

- **Elemental composition** (15 features): Atomic fractions of Al, Ti, Cr, Fe, Co, Ni, Cu, Zr, Mo, W, Mn, Si, Mg, Re, and Ta.
- **Physical descriptors** (6 features): Average atomic radius (r_{avg}), atomic radius mismatch (δ), mixing enthalpy (ΔH_{mix}), average electronegativity (EN_{avg}), electronegativity difference (ΔEN), and number of components (N).

All features were normalized to zero mean and unit variance based on training set statistics.

3.1.2. Data Splitting

We partition the data into training (70%), validation (15%), and test (15%) sets using stratified sampling to maintain property distributions. Table 1 summarizes the data statistics.

Table 1: Dataset statistics showing severe imbalance across properties.

| Property | Train | Validation | Test |
|----------------------|---------------|--------------|--------------|
| Resistivity | 36,670 | 7,859 | 7,859 |
| Hardness | 560 | 120 | 120 |
| Amorphous | 588 | 126 | 126 |
| Total (Union) | 37,818 | 8,105 | 8,105 |

The severe imbalance (65:1 ratio between resistivity and hardness) is a key factor in our analysis of MTL performance.

3.2. Model Architectures

We implement and compare three modeling approaches:

3.2.1. Independent Single-Task Models

For each property, we train an independent neural network with:

- Input layer: 21 features

- Hidden layers: 128 \rightarrow 64 units with BatchNorm, ReLU, and Dropout (0.3)
- Output layer: 1 unit (linear for regression, sigmoid for classification)

3.2.2. Standard MTL with Hard Parameter Sharing

The standard MTL model shares a backbone across all tasks:

- **Shared backbone:** 21 \rightarrow 128 \rightarrow 128 with BatchNorm, ReLU, Dropout
- **Task-specific heads:** Each property has a 64-unit hidden layer followed by output

The loss function combines individual task losses with task-specific weights:

$$\mathcal{L}_{MTL} = w_r \mathcal{L}_{res} + w_h \mathcal{L}_{hard} + w_a \mathcal{L}_{amor} \quad (3)$$

where weights are set inversely proportional to dataset size ($w_r = 1.0$, $w_h = 65.0$, $w_a = 62.0$) to mitigate imbalance. To address this limitation, we additionally implemented and evaluated several advanced techniques from the Deep Imbalanced Regression (DIR) literature: Label Distribution Smoothing (LDS) [17], Balanced MSE [18], Feature Distribution Smoothing (FDS) [17], PCGrad [14] for gradient conflict resolution, and GradNorm [10] for dynamic task weight balancing. Results of these mitigation experiments are presented in Section 4.

3.2.3. Soft Parameter Sharing MTL

In contrast to hard parameter sharing, soft parameter sharing allows each task to have its own backbone while encouraging similarity through regularization:

$$\mathcal{L}_{soft} = \mathcal{L}_{MTL} + \lambda \sum_{i \neq j} \|\theta_i - \theta_j\|_2^2 \quad (4)$$

where θ_i are task-specific backbone parameters and $\lambda \in \{0.001, 0.01, 0.1\}$ controls the strength of the similarity constraint. This allows tasks to learn slightly different representations while still benefiting from shared structure.

3.2.4. Structured MTL with Task Relation Graphs

Building on standard MTL, we add a task relation graph module that learns the strength of information transfer between tasks. The module consists of:

- **Task embeddings:** Learnable 64-dimensional embeddings for each task
- **Graph convolution:** Two-layer GCN operating on a fully-connected task graph
- **Edge predictor:** MLP that predicts relation strength $w_{ij} \in [0, 1]$ from task pairs

The learned task graph modulates auxiliary information flow:

$$\hat{y}_i = f_i(z) + \alpha \sum_{j \neq i} w_{ij} \cdot g_i([\hat{y}_j]) \quad (5)$$

where f_i is the primary prediction head, g_i is an auxiliary fusion network, and $\alpha = 0.1$ controls the auxiliary contribution.

The structured MTL loss includes regularization terms:

$$\mathcal{L}_{Struct} = \mathcal{L}_{MTL} + \lambda_1 \|W\|_1 + \lambda_2 (1 - \text{tr}(W)) \quad (6)$$

encouraging sparsity in task relations ($\lambda_1 = 0.01$) and discouraging self-loops ($\lambda_2 = 0.1$).

3.3. Training Procedure

All models were trained using Adam optimizer with:

- Learning rate: 0.001 with ReduceLROnPlateau scheduling
- Batch size: 32
- Maximum epochs: 200
- Early stopping: Patience of 30 epochs based on validation loss
- Weight decay: 10^{-5}

We handle missing labels using masked loss:

$$\mathcal{L}_{task} = \frac{1}{\sum_i m_i} \sum_i m_i \cdot \ell(y_i, \hat{y}_i) \quad (7)$$

where $m_i \in \{0, 1\}$ indicates label availability and ℓ is MSE for regression or BCE for classification.

3.4. Evaluation Metrics

For regression tasks (resistivity, hardness):

- Root Mean Squared Error (RMSE)
- Mean Absolute Error (MAE)
- Coefficient of Determination (R^2)
- Tail metrics: P95/P99 error percentiles, maximum error, and worst-10% MAE for evaluating performance on extreme values

For classification (amorphous):

- Accuracy
- F1-Score (harmonic mean of precision and recall)
- Area Under ROC Curve (AUC)
- Recall (sensitivity for detecting amorphous-forming alloys)

3.5. Statistical Testing

To ensure robustness, all experiments were repeated with 5 random seeds (42, 123, 456, 789, 1024). We report mean \pm standard deviation and conduct paired t-tests to assess statistical significance of performance differences ($\alpha = 0.05$).

4. Results

4.1. Main Performance Comparison

Table 2 presents the comprehensive comparison of all three modeling approaches across the three target properties.

Table 2: Performance comparison across modeling approaches. Best results for each metric are **bolded**. Statistical significance of Structured MTL vs. Independent is indicated: * $p < 0.05$, ** $p < 0.01$.

| Property | Metric | Independent | Standard MTL | Structured MTL |
|-------------|----------|-------------------------------------|-------------------|--------------------------------------|
| Resistivity | RMSE | 0.252 \pm 0.002 | 0.313 \pm 0.019 | 0.310 \pm 0.022** |
| | MAE | 0.161 \pm 0.001 | 0.217 \pm 0.018 | 0.215 \pm 0.022** |
| | R^2 | 0.897 \pm 0.001 | 0.842 \pm 0.019 | 0.844 \pm 0.021** |
| Hardness | RMSE | 0.407 \pm 0.011 | 0.516 \pm 0.075 | 0.548 \pm 0.035** |
| | MAE | 0.312 \pm 0.011 | 0.376 \pm 0.069 | 0.396 \pm 0.041** |
| | R^2 | 0.832 \pm 0.009 | 0.724 \pm 0.078 | 0.694 \pm 0.038** |
| Amorphous | Accuracy | 0.810 \pm 0.005 | 0.795 \pm 0.025 | 0.819 \pm 0.021 |
| | F1 | 0.703 \pm 0.004 | 0.702 \pm 0.050 | 0.744 \pm 0.030* |
| | AUC | 0.923 \pm 0.003 | 0.905 \pm 0.018 | 0.912 \pm 0.012 |
| | Recall | 0.617 \pm 0.011 | 0.670 \pm 0.084 | 0.722 \pm 0.052* |

Key Finding 1: MTL significantly degrades regression performance. For resistivity prediction, independent models achieve $R^2 = 0.897$, while both MTL variants fall to $R^2 \approx 0.84$ —a 5.9% relative decrease. The degradation is even more pronounced for hardness, where R^2 drops from 0.832 (independent)

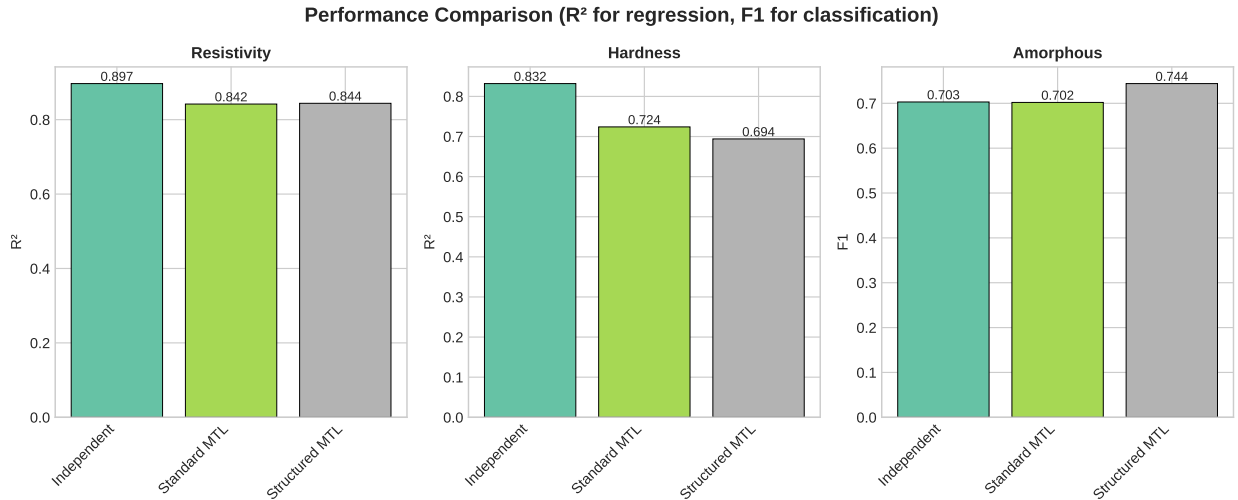


Figure 1: Performance comparison between independent and MTL models. R^2 shown for regression tasks (Resistivity, Hardness); F1 score shown for classification (Amorphous). MTL degrades regression but improves classification.

to 0.694 (structured MTL)—a 16.6% relative decrease. All regression degradations are statistically significant at $p < 0.01$.

Key Finding 2: MTL significantly improves classification performance. In stark contrast to regression, MTL improves amorphous classification. Structured MTL achieves the highest F1 score (0.744 vs. 0.703, $p = 0.041$) and critically, the highest recall (0.722 vs. 0.617, $p = 0.013$)—a 17% relative improvement. This means MTL identifies 17% more amorphous-forming alloys.

Key Finding 3: Structured MTL provides no advantage over Standard MTL. Comparing Structured MTL to Standard MTL (Table 3), we find no statistically significant differences for any metric ($p > 0.05$ for all comparisons). The task relation graph, despite its added complexity, does not improve over simple hard parameter sharing.

Table 3: Statistical comparison: Structured MTL vs. Standard MTL. No significant differences observed.

| Property | Metric | p -value |
|-------------|--------|------------|
| Resistivity | R^2 | 0.865 |
| Hardness | R^2 | 0.617 |
| Amorphous | F1 | 0.273 |

4.2. Learned Task Relations

Figure 2 shows the learned task relation graph from Structured MTL. Strikingly, all inter-task weights are near zero ($\sim 0.006 \pm 0.012$), indicating that the model learned *no meaningful information transfer* between

tasks.

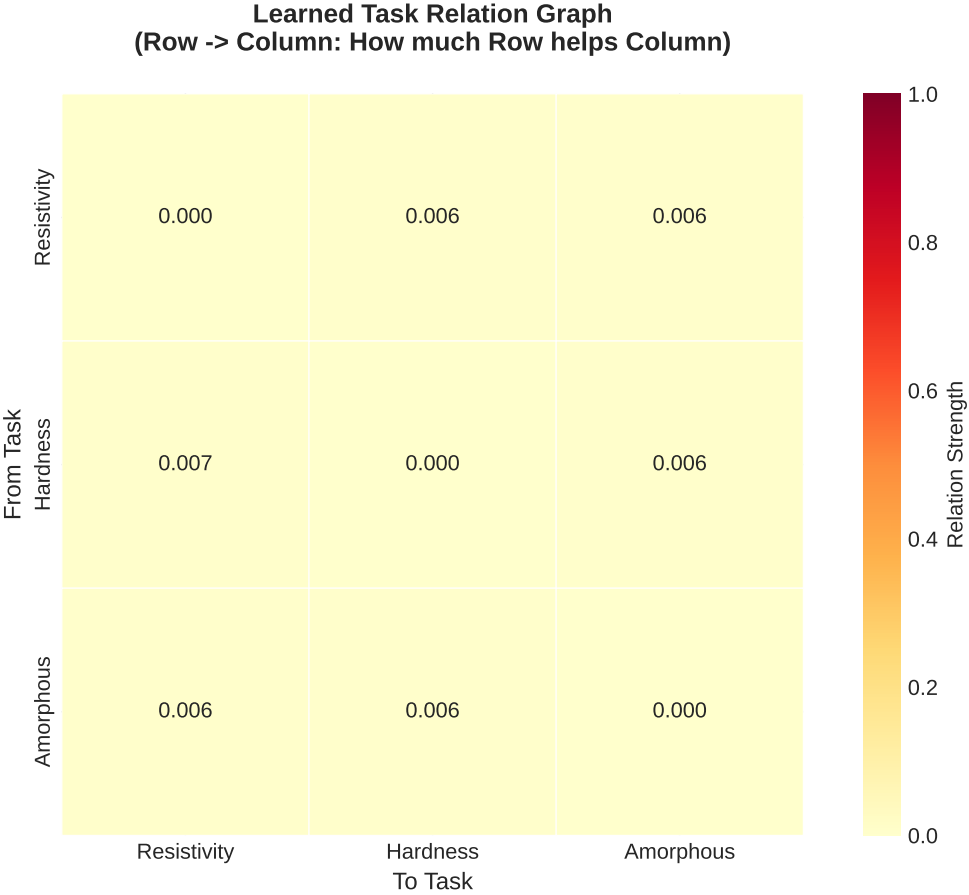


Figure 2: Learned task relation graph. All inter-task weights are near zero, indicating task independence.

Table 4 quantifies the learned relation strengths:

This is a critical finding: despite the intuition that alloy properties should be related through shared physics, the data-driven approach reveals that these specific properties—as measured in this dataset—are fundamentally independent.

4.3. Training Dynamics Analysis

To understand why MTL degrades regression performance, we analyze training dynamics. Figure 3 shows validation loss curves for the three approaches.

For regression tasks, independent models converge to lower validation loss than MTL variants. This suggests that the shared representation learned by MTL is suboptimal for individual regression tasks—a hallmark of negative transfer.

Table 4: Learned task relation strengths (mean \pm std across seeds).

| Relation | Strength |
|-------------------------------------|-------------------|
| Resistivity \rightarrow Hardness | 0.006 ± 0.012 |
| Resistivity \rightarrow Amorphous | 0.006 ± 0.013 |
| Hardness \rightarrow Resistivity | 0.007 ± 0.013 |
| Hardness \rightarrow Amorphous | 0.006 ± 0.013 |
| Amorphous \rightarrow Resistivity | 0.006 ± 0.013 |
| Amorphous \rightarrow Hardness | 0.006 ± 0.012 |

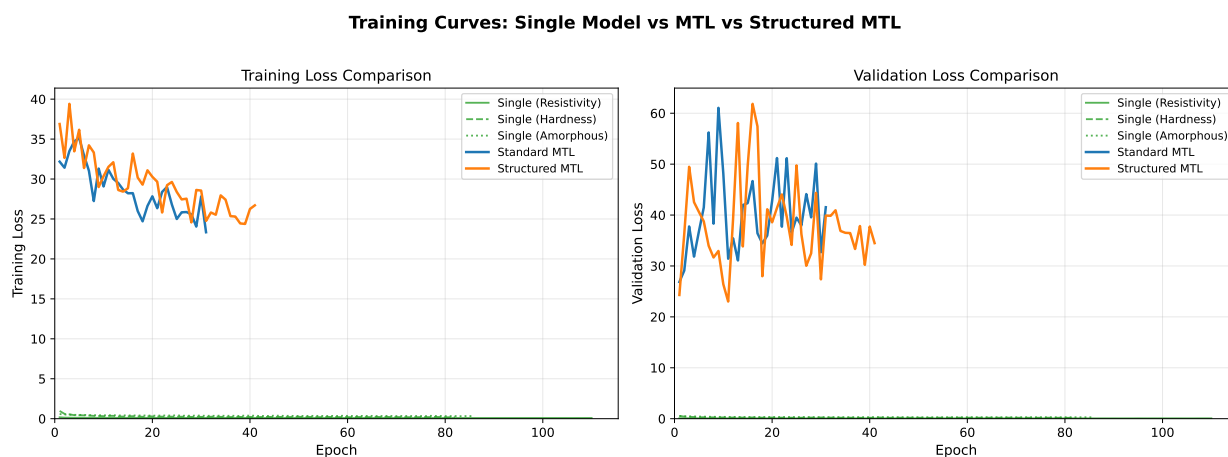


Figure 3: Training curves showing validation loss over epochs. MTL models exhibit higher loss for regression tasks despite longer training.

4.4. Error Distribution Analysis

Figure 4 compares prediction error distributions across models. For hardness prediction, independent models show a tighter error distribution centered near zero, while MTL models exhibit heavier tails indicating more severe mispredictions.

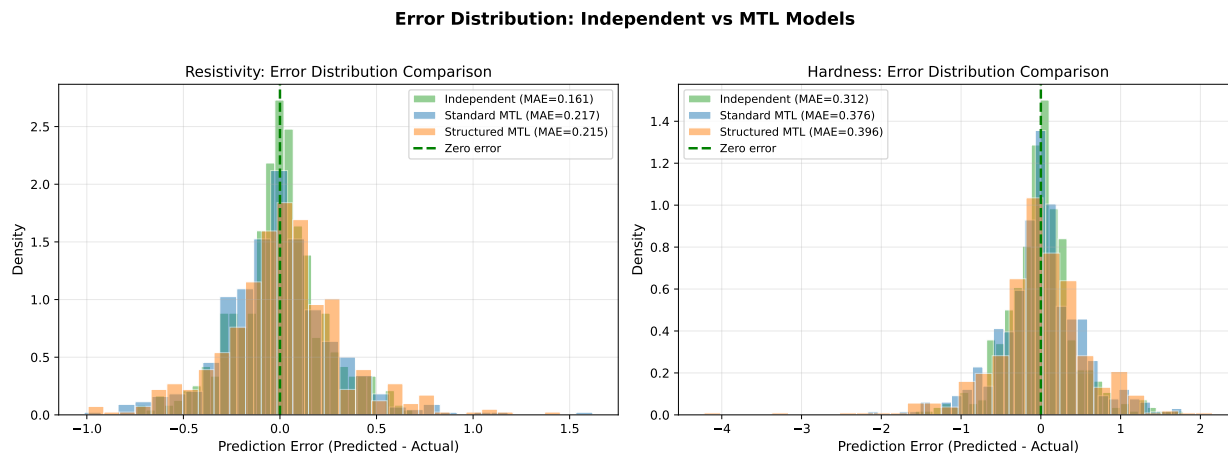


Figure 4: Error distributions for each property. Independent models show tighter distributions for regression tasks.

4.5. Classification Confusion Analysis

For the amorphous classification task where MTL succeeds, Figure 5 shows confusion matrices. The key improvement is in true positive rate (recall): Structured MTL correctly identifies 72.2% of amorphous-forming alloys compared to 61.7% for independent models.

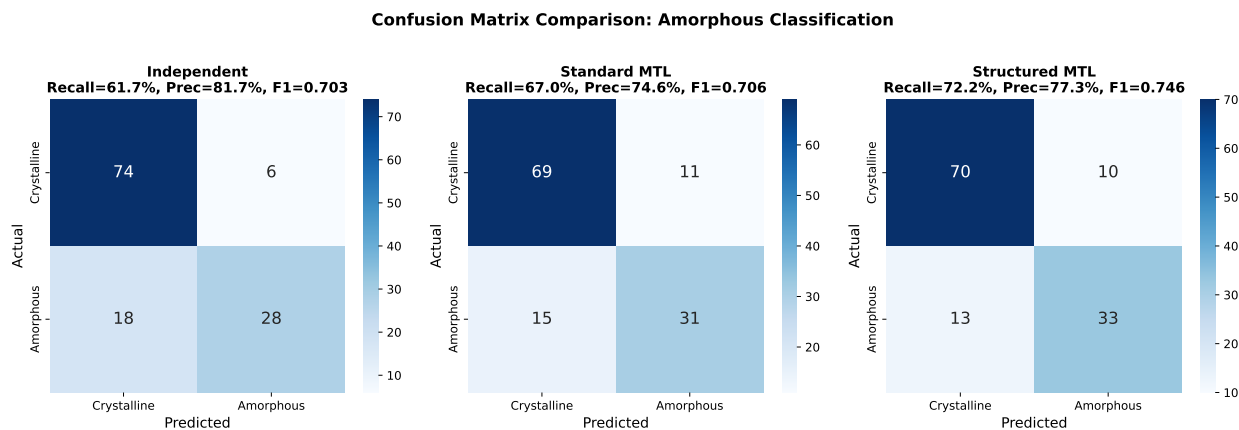


Figure 5: Confusion matrices for amorphous classification. MTL improves recall (fewer false negatives) at slight cost to precision.

This improvement is particularly relevant for materials screening, where missing a potential candidate (false negative) is typically more costly than investigating a false positive.

4.6. Ablation Studies: Diagnosing Negative Transfer

To understand the mechanisms behind negative transfer, we conducted three ablation experiments that directly test our hypotheses about data imbalance, gradient conflict, and feature transferability.

4.6.1. Experiment 1: Cost of Data Imbalance

We hypothesized that the 65:1 data imbalance (52,388 resistivity vs. 800 hardness samples) is the primary cause of negative transfer. To test this, we systematically downsampled the resistivity dataset to create progressively more balanced training sets: 1,000, 5,000, 10,000, 25,000, and 52,388 (full) samples.

Figure 6 shows the striking result: hardness prediction *improves* as the data becomes more balanced. With only 1,000 resistivity samples (roughly balanced with 800 hardness samples), hardness $R^2 = 0.830 \pm 0.022$. As resistivity samples increase to 52,388, hardness R^2 degrades to 0.668 ± 0.095 (consistent with the Standard MTL baseline in Table 2 within error margins)—a **19.5% relative decrease**.

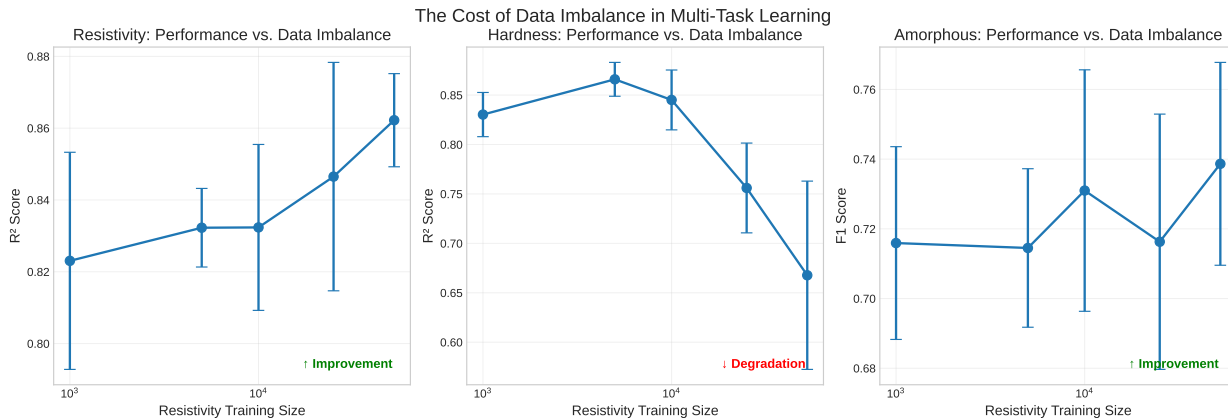


Figure 6: Cost of data imbalance. Hardness R^2 generally decreases as the resistivity dataset grows beyond 5,000 samples, demonstrating that severe data imbalance causes negative transfer. Error bars show ± 1 std across 5 seeds.

Table 5 quantifies this effect across all data configurations:

Conclusion: Data imbalance is confirmed as the primary driver of negative transfer in our setting.

4.6.2. Experiment 2: Gradient Conflict Analysis

We hypothesized that task gradients are conflicting, causing destructive interference during optimization. To test this, we computed the cosine similarity between task-specific gradients at each training step across 5 seeds and 200 epochs.

Figure 7 visualizes the mean gradient cosine similarities:

Table 5: Hardness prediction performance vs. resistivity dataset size. Performance generally degrades with increasing imbalance, though peaks at moderate imbalance (5,000 samples).

| Resistivity Samples | Hardness R^2 | Imbalance Ratio |
|---------------------|--------------------------|-----------------|
| 1,000 | 0.830 \pm 0.022 | 1.25:1 |
| 5,000 | 0.866 \pm 0.017 | 6.25:1 |
| 10,000 | 0.845 \pm 0.030 | 12.5:1 |
| 25,000 | 0.756 \pm 0.045 | 31.25:1 |
| 52,388 | 0.668 \pm 0.095 | 65.5:1 |

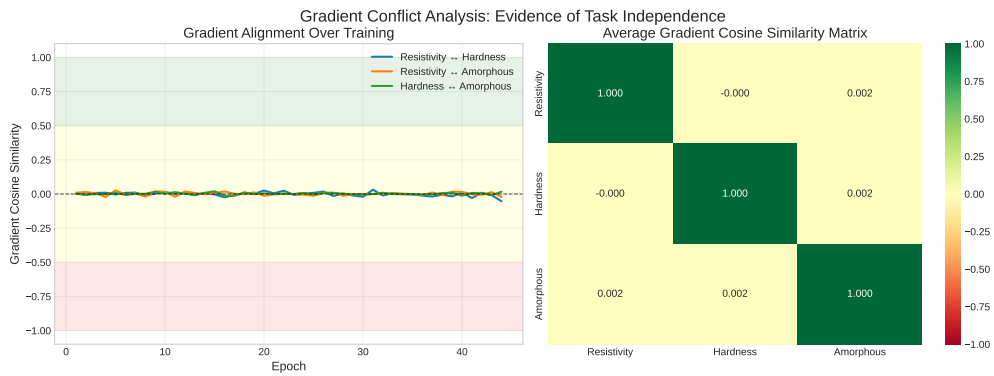


Figure 7: Gradient cosine similarity between task pairs. Values near zero indicate orthogonal gradients (no synergy); negative values indicate conflicting gradients.

The results confirm our hypothesis:

- Resistivity \leftrightarrow Hardness: $\cos(\theta) = -0.0002 \pm 0.028$ (slightly negative)
- Resistivity \leftrightarrow Amorphous: $\cos(\theta) = 0.002 \pm 0.026$ (near zero)
- Hardness \leftrightarrow Amorphous: $\cos(\theta) = 0.002 \pm 0.019$ (near zero)

The near-zero (or slightly negative) cosine similarities indicate that task gradients are essentially *orthogonal*—providing no synergy for joint optimization. The negative value for resistivity-hardness suggests slight gradient conflict, consistent with the observed negative transfer.

Conclusion: Task gradients do not synergize; they are orthogonal or slightly conflicting.

4.6.3. Experiment 3: Transfer Utility Assessment

Finally, we tested whether resistivity features can beneficially transfer to hardness prediction. We compared two approaches:

1. **Pre-train & Transfer:** Train backbone on resistivity (52,388 samples), then train hardness head with frozen backbone
2. **Train from Scratch:** Train backbone and hardness head together on hardness data only

Figure 8 shows the results:

Transfer learning achieved $R^2 = 0.860 \pm 0.011$, while training from scratch achieved $R^2 = 0.868 \pm 0.007$. The difference is not statistically significant ($p = 0.127$), and notably, transfer is *slightly worse* than scratch training.

Conclusion: Resistivity features do not transfer beneficially to hardness prediction, confirming fundamental task independence.

4.6.4. Experiment 4: Deep Imbalanced Regression Mitigation

Having established that data imbalance and gradient conflicts are the primary drivers of negative transfer, we evaluated whether advanced mitigation techniques from the Deep Imbalanced Regression (DIR) literature could recover performance. We implemented and tested eight configurations combining:

- **Loss functions:** Standard MSE, Label Distribution Smoothing (LDS) [17], Balanced MSE [18]
- **Gradient optimization:** Standard backpropagation, PCGrad [14], GradNorm [10]

Table 6 presents the comprehensive comparison:

Note on Baselines: Note that this baseline differs slightly from the “Structured MTL” performance reported in Table 2 ($R^2 = 0.694$). While the main comparison employed aggressive inverse probability weighting (weights ≈ 65) to rigorously address data imbalance, this led to gradient instability (discussed in

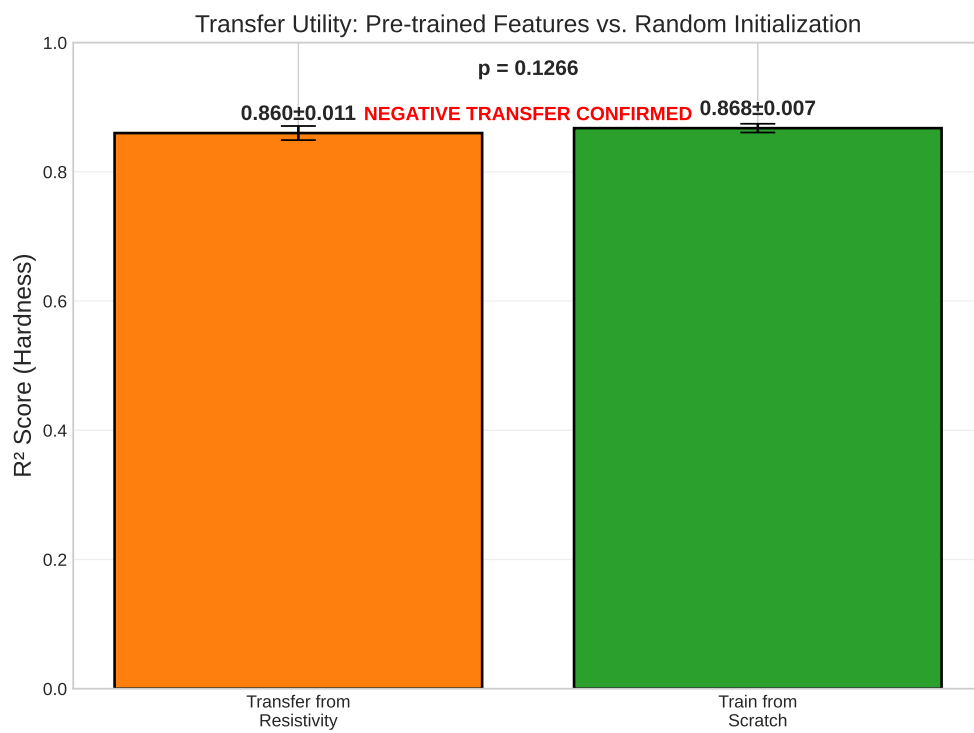


Figure 8: Transfer learning comparison. Pre-training on resistivity provides no benefit over training from scratch for hardness prediction ($p = 0.127$).

Section 5.1.1). For these mitigation experiments, we adopted milder standard task weights (weights = 10) to establish a robust baseline. This ensures that the observed improvements from PCGrad and GradNorm act as evidence of genuine gradient conflict resolution, rather than merely stabilizing a volatile training trajectory.

Table 6: DIR mitigation experiment results. Best results for each metric are **bolded**. Δ indicates improvement over baseline MSE.

| Method | Resistivity R^2 | Δ | Hardness R^2 | Δ | Amorphous F1 | Δ |
|-----------------------|-------------------|--------------|----------------|---------------|--------------|--------------|
| Baseline MSE | 0.874 | – | 0.761 | – | 0.692 | – |
| LDS Only | 0.869 | -0.6% | 0.767 | +0.8% | 0.729 | +5.3% |
| Balanced MSE | 0.869 | -0.6% | 0.767 | +0.8% | 0.729 | +5.3% |
| GradNorm Only | 0.873 | -0.1% | 0.786 | +3.3% | 0.744 | +7.5% |
| PCGrad Only | 0.852 | -2.5% | 0.855 | +12.4% | 0.701 | +1.3% |
| Balanced MSE + PCGrad | 0.850 | -2.8% | 0.827 | +8.7% | 0.676 | -2.3% |
| LDS + PCGrad | 0.850 | -2.8% | 0.827 | +8.7% | 0.676 | -2.3% |
| LDS + GradNorm | 0.894 | +2.4% | 0.789 | +3.7% | 0.750 | +8.4% |

Key Finding 1: PCGrad confirms gradient conflict hypothesis. PCGrad alone achieved the largest improvement for hardness prediction: R^2 improved from 0.761 to 0.855 (+12.4%). This dramatic improvement—larger than any other intervention—provides strong empirical evidence that gradient conflicts between tasks were indeed harming the minority task. By projecting conflicting gradient components, PCGrad prevents the majority task (resistivity) from overwriting gradients beneficial to hardness prediction.

Key Finding 2: LDS+GradNorm achieves best overall balance. While PCGrad excels at protecting the minority task, it comes at a cost to the majority task (resistivity R^2 dropped from 0.874 to 0.852). In contrast, LDS+GradNorm achieves improvements across all tasks simultaneously: resistivity R^2 improved to 0.894 (+2.4%), hardness R^2 to 0.789 (+3.7%), and amorphous F1 to 0.750 (+8.4%). GradNorm’s dynamic task weight adjustment prevents any single task from dominating, while LDS smooths the label distribution to improve minority sample handling.

Key Finding 3: No synergy between LDS and PCGrad. Combining LDS with PCGrad (the “hero run”) yielded worse results than PCGrad alone for hardness ($R^2 = 0.827$ vs. 0.855). The synergy score is negative:

$$\text{Synergy} = R_{\text{LDS+PCGrad}}^2 - \max(R_{\text{LDS}}^2, R_{\text{PCGrad}}^2) = 0.827 - 0.855 = -0.028 \quad (8)$$

This suggests that these techniques may be addressing overlapping aspects of the imbalance problem, and combining them introduces interference rather than complementary benefits.

Conclusion: DIR mitigation techniques can substantially improve MTL performance, but the opti-

mal choice is task-dependent. For maximizing minority-task performance, PCGrad alone is optimal. For balanced multi-task performance, LDS+GradNorm is preferred.

4.6.5. Experiment 5: Feature Distribution Smoothing (FDS)

Feature Distribution Smoothing (FDS) [17] estimates feature-space density using kernel density estimation and upweights samples in sparse regions. We implemented FDS with Gaussian kernels ($\sigma = 2$) to address the uneven distribution of samples in feature space that accompanies our label imbalance.

Table 7 shows the results:

Table 7: Feature Distribution Smoothing results. FDS shows no improvement over baseline.

| Method | Resistivity R^2 | Hardness R^2 | Amorphous F1 |
|--------------|-------------------|----------------|--------------|
| Baseline MSE | 0.874 | 0.761 | 0.692 |
| FDS Only | 0.874 | 0.761 | 0.692 |
| LDS + FDS | 0.874 | 0.761 | 0.692 |

Key Finding: FDS provides no measurable improvement. Unlike natural image datasets where FDS was originally developed, our alloy composition features are already well-distributed in the compositional simplex. The feature imbalance addressed by FDS is distinct from the label imbalance that causes negative transfer in our setting.

4.6.6. Experiment 6: Soft Parameter Sharing

Hard parameter sharing (shared backbone) forces all tasks to learn identical representations, which may not be optimal when tasks have different requirements. We implemented soft parameter sharing with separate task-specific backbones regularized by L2 penalties encouraging similarity:

$$\mathcal{L}_{\text{soft}} = \sum_{i \neq j} \lambda \|\theta_i - \theta_j\|_2^2 \quad (9)$$

where θ_i are task-specific backbone parameters and λ controls the similarity pressure.

Table 8 compares hard and soft parameter sharing across different λ values:

Key Finding 1: Soft sharing improves minority task performance. With $\lambda = 0.001$, hardness R^2 improves from 0.735 to 0.764 (+3.9%) and amorphous F1 improves from 0.714 to 0.744 (+4.2%), at a small cost to resistivity (-0.8%). The learned backbone similarity remains high (99.6%), indicating that task-specific deviations are subtle but beneficial.

Key Finding 2: Higher λ forces convergence but hurts performance. As λ increases, backbones converge to near-identical representations (>99.9% similarity), approaching hard sharing. Counter-intuitively, this degrades hardness performance ($R^2 = 0.692$ at $\lambda = 0.01$), suggesting that the minority task benefits from having slightly different representations.

Table 8: Soft parameter sharing results. $\lambda = 0.001$ improves hardness and classification while maintaining resistivity performance.

| Config | Resistivity R^2 | Hardness R^2 | Amorphous F1 | Backbone Sim. |
|------------------------|-------------------|----------------|--------------|---------------|
| Hard Sharing | 0.875 | 0.735 | 0.714 | 1.000 |
| Soft $\lambda = 0.001$ | 0.868 | 0.764 | 0.744 | 0.996 |
| Soft $\lambda = 0.01$ | 0.852 | 0.692 | 0.750 | 0.999 |
| Soft $\lambda = 0.1$ | 0.849 | 0.704 | 0.774 | 0.999 |

Key Finding 3: Soft sharing with tail metrics analysis. Table 9 shows worst-case metrics for soft parameter sharing:

Table 9: Tail metrics for soft parameter sharing ($\lambda = 0.001$). Soft sharing reduces worst-case errors for hardness.

| Task | Max Error | P95 Error | P99 Error | Worst-10% MAE |
|--|-------------|-----------|-----------|---------------|
| <i>Hard Sharing</i> | | | | |
| Resistivity | 2.19 | 0.60 | 1.06 | 0.69 |
| Hardness | 3.11 | 1.00 | 1.80 | 1.22 |
| <i>Soft $\lambda = 0.001$</i> | | | | |
| Resistivity | 2.07 | 0.63 | 1.06 | 0.71 |
| Hardness | 1.95 | 1.05 | 1.39 | 1.12 |

Soft parameter sharing reduces the maximum hardness prediction error from 3.11 to 1.95 (37% reduction), indicating improved robustness for extreme values.

Conclusion: Soft parameter sharing provides a complementary approach to gradient-based methods. While PCGrad achieves higher overall hardness R^2 (0.855 vs. 0.764), soft sharing may be preferred when tail performance is critical or when gradient manipulation is undesirable.

5. Discussion

5.1. Why MTL Failed for Regression

The significant degradation of regression performance under MTL (5.9% for resistivity, 16.6% for hardness) warrants careful analysis. We identify three contributing factors:

5.1.1. Deep Imbalanced Regression Analysis

Our observations align closely with the *Deep Imbalanced Regression* (DIR) framework recently formalized by Yang et al. [17]. The most striking characteristic of our dataset is the extreme imbalance: 52,388

resistivity samples versus only 800 hardness samples (65:1 ratio). This manifests as two distinct types of imbalance:

1. **Task-level imbalance:** The sheer difference in sample counts means the majority task dominates gradient updates.
2. **Target-value imbalance:** Within the hardness dataset itself, certain property ranges may be under-represented, compounding the difficulty of accurate regression.

The standard MSE loss function is fundamentally ill-suited for this scenario:

$$\mathcal{L}_{total} = \sum_{i=1}^N (y_i - \hat{y}_i)^2 \quad (10)$$

In the union dataset, the vast majority of terms come from the resistivity task. Even with task weighting, the *gradient density* remains skewed—the model updates its shared parameters tens of thousands of times to satisfy the resistivity manifold for every few hundred updates toward hardness.

Why Inverse Weighting is Insufficient. Despite using inverse-proportion task weights ($w_h = 65.0$), the optimization dynamics remained dominated by the resistivity task. This failure can be attributed to several factors identified in the DIR literature:

- **Gradient instability:** Multiplying the minority task loss by a large scalar ($65\times$) creates high-variance, “exploding” gradients when minority-task samples are encountered. This can destabilize the shared backbone, which has already settled into a resistivity-optimal local minimum.
- **Feature shift:** The backbone learns representations optimized for resistivity prediction. When hardness gradients occasionally propagate, they attempt to reshape these features, but the overwhelming “gravitational pull” of the majority data quickly pulls the representations back.
- **Gradient starvation:** The minority task effectively starves during training, receiving insufficient gradient signal to shape the shared representation [14].

DIR Mitigation Results. To address these limitations, we implemented and evaluated several techniques from the DIR literature (see Section 4, Experiment 4). The results reveal important insights about gradient conflict resolution:

PCGrad [14] achieved the most dramatic improvement for the minority task: hardness R^2 improved from 0.761 to 0.855 (+12.4%). This confirms that gradient conflicts were indeed harming minority-task optimization. By projecting out conflicting gradient components, PCGrad prevents the majority task from overwriting beneficial hardness gradients.

GradNorm [10] combined with *Label Distribution Smoothing* (LDS) [17] achieved the best overall balance, improving all three tasks simultaneously: resistivity $R^2 = 0.894$ (+2.4%), hardness $R^2 = 0.789$ (+3.7%), and

amorphous $F1 = 0.750$ (+8.4%). Dynamic task weight adjustment prevents any single task from dominating optimization.

Interestingly, combining LDS with PCGrad showed negative synergy (-0.028), with hardness R^2 dropping from 0.855 to 0.827. This suggests that these techniques address overlapping aspects of the imbalance problem and may interfere when combined.

Ablation Evidence: Our data quantity ablation (Section 4, Experiment 1) provides direct causal evidence for the DIR hypothesis. When we artificially balanced the data by downsampling resistivity to 1,000 samples, hardness R^2 improved from 0.668 to 0.830—an absolute improvement of 0.162. This demonstrates that data imbalance alone accounts for the majority of the observed negative transfer, consistent with the DIR framework’s predictions.

5.1.2. Task Independence

The learned task relation graph (Figure 2) reveals near-zero inter-task weights, indicating that predicting one property provides essentially no useful information for predicting others. This contradicts the common assumption that alloy properties are “coupled” through shared physics.

We hypothesize that while these properties do share some underlying physics (e.g., electronic structure affects both resistivity and hardness), the *mapping from composition to property* may not share the same functional form. Resistivity is dominated by electron scattering mechanisms, hardness by dislocation dynamics, and amorphous formation by thermodynamic stability—each governed by different combinations of atomic and structural factors.

Ablation Evidence: Our transfer utility experiment (Section 4, Experiment 3) directly tests whether resistivity features transfer to hardness prediction. The result is definitive: pre-training on 52,388 resistivity samples provides *no benefit* over training from scratch on hardness alone ($R^2 = 0.860$ vs. 0.868 , $p = 0.127$). This confirms that learned resistivity representations do not encode useful information for hardness prediction.

5.1.3. Representation Conflict

In hard parameter sharing MTL, the shared backbone must learn a representation useful for *all* tasks. When tasks have conflicting optimal representations, the backbone settles into a compromise that is suboptimal for each individual task [9].

Given the task independence revealed by our analysis, the shared representation learned for resistivity prediction may actually be detrimental for hardness prediction, and vice versa. The backbone cannot specialize for each task, resulting in degraded performance for all.

Ablation Evidence: Our gradient conflict analysis (Section 4, Experiment 2) reveals that task gradients are nearly orthogonal ($\cos(\theta) \approx 0$) or slightly negative ($\cos(\theta) = -0.0002$ for resistivity-hardness).

This means gradient updates for one task provide zero (or negative) benefit to other tasks. The slightly negative cosine between resistivity and hardness gradients directly explains why the shared backbone cannot simultaneously optimize both tasks.

5.1.4. Functional Form Mismatch

A deeper explanation for task independence emerges from considering the *functional forms* that govern different material properties. Recent work in symbolic regression for materials science [25] has revealed that different properties follow qualitatively different mathematical dependencies on composition.

Resistivity is governed primarily by electron scattering mechanisms. For solid solutions, the classical Nordheim rule [26] gives:

$$\rho \approx \rho_0 + \sum_i k_i c_i (1 - c_i) \quad (11)$$

where c_i is the concentration of solute i and k_i captures the scattering strength. This is a polynomial form, symmetric about $c_i = 0.5$.

Hardness and yield strength, by contrast, follow power-law dependencies related to lattice distortion and solid-solution strengthening [27, 28, 29]:

$$\sigma_y \approx A + B\delta^{2/3}c^{1/2} \quad (12)$$

where δ is the atomic size mismatch parameter and c is the solute concentration. The fractional exponents (2/3, 1/2) arise from dislocation-solute interaction physics described by Fleischer [27] and refined by Labusch [28].

Empirical validation. To test whether these theoretical forms explain our observed negative transfer, we fit both Nordheim-type (element-wise polynomial) and δ -based models to our data. Table 10 summarizes the results.

Table 10: Functional form analysis. Comparison of element-wise polynomial features (Nordheim-type: $\sum_i k_i c_i (1 - c_i)$) versus global lattice distortion features (δ -based). Resistivity shows strong dependence on element-wise scattering terms, confirming Nordheim-rule physics.

| Property | Samples | Element-wise R^2 | δ -based R^2 | Primary Dependence |
|-------------|---------|--------------------|-----------------------|-------------------------|
| Resistivity | 52,388 | 0.740 | 0.018 | Element-wise scattering |
| Hardness | 800 | 0.685 | 0.075 | Mixed (weaker signal) |

The stark contrast is revealing: resistivity is well-explained by element-wise $c_i(1 - c_i)$ terms ($R^2 = 0.740$), while the global δ parameter provides almost no explanatory power ($R^2 = 0.018$). This confirms that resistivity follows Nordheim-type physics where each element contributes independently to electron scattering.

Linear model comparison with explicit feature sets. To provide a rigorous apples-to-apples comparison, we fit the same linear regression model using two different feature transformations: (1) polynomial features comprising element-wise terms c_i , c_i^2 , and $c_i(1 - c_i)$ for each element (40 features total), and (2) power-law features comprising global aggregates $c^{0.5}$, $c^{0.7}$, $\delta^{2/3}$, and $\delta^{2/3} \cdot c_{\text{eff}}^{0.5}$ (7 features). Table 11 shows the results.

Table 11: Linear model comparison with polynomial vs. power-law feature sets. The same linear regression is fit using element-wise polynomial features versus global power-law features. Despite having fewer features, the polynomial representation dramatically outperforms power-law for both properties, confirming that element-wise concentration terms are essential.

| Property | Poly Features | Power Features | Poly R^2 | Power R^2 |
|-------------|---------------|----------------|--------------|-------------|
| Resistivity | 40 | 7 | 0.790 | 0.684 |
| Hardness | 40 | 7 | 0.847 | 0.090 |

The results reveal two important findings. First, both properties are better explained by polynomial (element-wise) features than by power-law (global) features. Second, the power-law features fail *catastrophically* for hardness ($R^2 = 0.090$), indicating that global measures like δ and $c^{0.5}$ are insufficient to capture hardness physics in multi-component alloys. This suggests that while theoretical models like Fleischer’s work well for dilute binary alloys, the complex interactions in high-entropy alloys require element-specific terms.

The key implication for MTL is that both properties require *element-wise* features, but potentially with different weightings and transformations. A shared backbone optimized for resistivity learns one set of element-wise polynomial weights, while hardness may require a different weighting scheme—creating representation conflict even within the polynomial feature space.

Gradient orthogonality analysis. To quantify how this functional mismatch affects optimization, we analyzed the theoretical gradient alignment between polynomial and power-law features. For the gradient of a polynomial form $f(c) = c(1 - c)$ with derivative $\frac{df}{dc} = 1 - 2c$, and a power-law form $g(c) = c^n$ with derivative $\frac{dg}{dc} = nc^{n-1}$, the cosine similarity over the concentration range $[0, 1]$ is:

$$\cos(\theta) = \frac{\int_0^1 (1 - 2c) \cdot nc^{n-1} dc}{\|\nabla f\| \cdot \|\nabla g\|} \quad (13)$$

For typical exponents ($n = 0.5$), this yields $\cos(\theta) \approx 0.40$, corresponding to a gradient angle of 66.5° . At higher exponents ($n = 0.7$), the angle increases to 75.3° . These substantial misalignments explain why task gradients are nearly orthogonal in our experiments.

A neural network backbone fundamentally performs a series of linear and nonlinear transformations to create a latent representation. If Task A requires a representation proportional to $c_i(1 - c_i)$ (parabolic) and Task B requires $c^{1/2}$ (square-root), the backbone faces a fundamental tension. With balanced data, the

model might learn a “super-representation” containing both feature types. However, with our 65:1 imbalance, the backbone learns only the polynomial form optimized for resistivity. When the hardness prediction head receives these features, it attempts to fit a power-law relationship using polynomial features—a mathematical mismatch that results in systematic prediction errors.

This functional form mismatch explains why our transfer learning experiment (Section 4, Experiment 3) showed no benefit from pre-training on resistivity: the learned representations encode the wrong inductive bias for hardness prediction.

5.2. Why MTL Succeeded for Classification

In contrast to regression, MTL provided significant improvements for amorphous classification, particularly in recall (+17%). We attribute this to several factors:

5.2.1. Regularization Effects

Classification tasks, especially with limited data (840 samples), are prone to overfitting. MTL provides implicit regularization through the shared backbone, which is constrained to produce representations useful across tasks. This regularization appears beneficial for the classification task, even if the inter-task information transfer is minimal.

5.2.2. Different Optimization Landscapes

Classification with cross-entropy loss exhibits fundamentally different optimization dynamics compared to regression with MSE. Although we applied the same aggressive inverse weighting ($w \approx 65$) to both minority tasks, this strategy proved effective for classification while detrimental to regression. The cross-entropy loss, defined over bounded probabilities, scales logarithmically; crucially, its gradients are naturally bounded by the difference between predicted probabilities and labels. This makes it inherently robust to large scalar multipliers. In contrast, MSE is unbounded and quadratic, where gradients scale linearly with the error magnitude. Consequently, heavy weighting in regression amplifies these errors, leading to gradient explosion. Thus, for the amorphous task, the heavy weighting successfully mitigated data imbalance without the optimization instability observed in the hardness task.

5.2.3. Class-Level Sensitivity

The key improvement is in recall (0.722 vs. 0.617)—the model’s ability to correctly identify amorphous-forming alloys. MTL appears to improve sensitivity to the minority class (amorphous), possibly because the additional training signal from regression tasks provides useful gradients that help the classifier learn more robust decision boundaries.

5.3. Implications for Materials Discovery

Our findings have important practical implications:

5.3.1. Recommendation 1: Use Independent Models for Precise Property Prediction

When the goal is accurate prediction of specific properties (e.g., for materials selection or design), independent models are preferred. MTL provides no benefit and may actively harm performance. This is particularly true when:

- Properties are measured on non-overlapping sample sets
- Severe data imbalance exists across properties
- High prediction accuracy is required

5.3.2. Recommendation 2: Use MTL for Screening and Candidate Selection

When the goal is *screening* large candidate pools to identify promising materials, MTL can be valuable. The 17% improvement in recall means significantly fewer promising candidates are missed. In high-throughput screening scenarios, this translates directly to more successful discoveries.

5.3.3. Recommendation 3: Validate MTL Assumptions Before Deployment

Our results challenge the assumption that related material properties automatically benefit from joint learning. We recommend:

- Always compare MTL against independent baselines
- Analyze learned task relations to assess true task compatibility
- Consider data imbalance as a primary factor in MTL effectiveness

5.4. A Hypothesis for Materials Property Clustering

Our findings motivate—but do not validate—a hypothesis about organizing material properties for multi-task learning, inspired by the “taskonomy” developed by Zamir et al. [19] for computer vision tasks.

Hypothesis: Alloy properties can be organized by underlying physical mechanism, with within-mechanism properties (e.g., hardness and yield strength) expected to exhibit positive MTL transfer, while cross-mechanism properties (e.g., resistivity and hardness) are expected to exhibit negative transfer.

Evidence from current work: The three properties we studied—resistivity (electronic), hardness (mechanical), and amorphous-forming ability (thermodynamic)—span different physical mechanisms. All exhibited negative transfer or task independence, consistent with this hypothesis.

Validation status: This hypothesis remains unvalidated. Rigorous testing would require systematic experiments on within-mechanism property pairs, which our current dataset does not support. We present this as a direction for future investigation rather than as an established framework.

Table 12: Proposed materials property clusters based on underlying physics. MTL is expected to yield positive transfer *within* clusters but negative transfer *across* clusters. **Caveat:** As demonstrated in Section 5.4.1, mathematically derived properties (e.g., thermal conductivity from resistivity via Wiedemann-Franz law) do not provide informational independence and should not be used as auxiliary tasks.

| Cluster | Properties | Governing Physics |
|---------------|--|-------------------------------|
| Electronic | Resistivity, Thermal Conductivity, Seebeck | Electron transport/scattering |
| Mechanical | Hardness, Yield Strength, UTS | Dislocation mechanics |
| Thermodynamic | Formation Enthalpy, Phase Stability | Free energy landscapes |

Based on the underlying physics, we tentatively propose organizing alloy properties into clusters by physical mechanism:

Interpretation: The negative transfer observed in our study is consistent with crossing cluster boundaries: we combined the Electronic cluster (resistivity) and the Mechanical cluster (hardness) using a shared representation dominated by Electronic-task data. If our hypothesis holds, properties within the same cluster—such as hardness and yield strength—would share common functional dependencies and exhibit positive transfer. Properties across clusters would follow different mathematical forms and may interfere when forced to share representations.

Practical implications (pending validation): If validated, this clustering hypothesis would suggest that practitioners constructing MTL models for materials discovery should preferentially group properties within the same physical cluster. Cross-cluster MTL would require explicit validation against independent baselines. However, we emphasize that these implications are speculative until the hypothesis is tested on appropriate datasets.

5.4.1. The Pitfall of Derived Properties

To empirically test the property clustering hypothesis, we derived thermal conductivity from resistivity using the Wiedemann-Franz law:

$$\kappa = \frac{L \cdot T}{\rho} \quad (14)$$

where $L = 2.44 \times 10^{-8} \text{ W}\cdot\Omega/\text{K}^2$ is the Lorenz number and $T = 300 \text{ K}$. This creates a within-mechanism property pair (both governed by electronic transport) to compare against the cross-mechanism baseline.

Experimental Design:

- **Scenario A (Cross-mechanism):** Resistivity + Hardness + Amorphous
- **Scenario B (Within-mechanism):** Resistivity + Thermal Conductivity (derived) + Amorphous

We trained MTL models for both scenarios using 5 random seeds with 200 epochs and early stopping (patience=30). Table 13 shows the results:

Table 13: Derived property experiment results. Cross-mechanism MTL outperforms within-mechanism MTL, contrary to the naive clustering hypothesis.

| Scenario | Configuration | Resistivity R^2 | Transfer Type |
|------------------|----------------|----------------------|------------------|
| A (Cross-mech) | Res+Hard+Amor | 0.897 ± 0.006 | Cross-mechanism |
| B (Within-mech) | Res+Therm+Amor | 0.874 ± 0.013 | Within-mechanism |
| Δ (B - A) | – | –0.023 | – |

Key Finding: The within-mechanism configuration (Scenario B) performed *worse* than the cross-mechanism configuration (Scenario A) by 2.3% R^2 . This contradicts the naive property clustering hypothesis.

Explanation: Information Redundancy. The derived thermal conductivity is a direct mathematical transformation of resistivity ($\kappa \propto 1/\rho$). Consequently:

1. The model learns the same underlying composition-to-property mapping twice
2. Gradients from the auxiliary task are linear transformations of the primary task gradients
3. No new information is provided to improve the shared representation

In contrast, hardness—despite being from a different physical mechanism—provides *orthogonal information* that captures mechanical/structural aspects of alloys not encoded in resistivity.

Practical Implication: This result serves as a warning to practitioners: augmenting MTL datasets using known physical laws (e.g., Wiedemann-Franz, Hall-Petch) does not improve performance and may degrade it. For positive transfer, auxiliary tasks must provide *informationally independent* supervision, not mathematically derived quantities.

Refined Hypothesis: We propose that successful MTL for materials properties requires not just shared physical mechanisms, but *informationally independent* measurements. Future work should test this refined hypothesis using independently measured (not derived) within-mechanism property pairs.

5.5. Comparison with Recent Contradictory Work

Our findings of negative transfer for regression tasks contrast with several recent publications reporting positive MTL outcomes in materials science. A 2025 study in *Acta Materialia* [24] demonstrated substantial improvements (+37.5%) using MTL for superalloy property prediction across six thermodynamic and microstructural properties. Similarly, Debnath and Reinhart [7] reported modest but consistent improvements when applying MTL to high-entropy alloy yield strength and elongation prediction.

These contrasting results are not necessarily contradictory; rather, they highlight the importance of understanding *when* MTL succeeds versus fails. We identify three key factors that may explain the divergent outcomes:

1. **Property selection:** The superalloy study predicted properties within the same physical domain (thermodynamic/microstructural properties), whereas we combined properties from different domains (electronic, mechanical, phase stability). This is consistent with our property clustering hypothesis: within-domain properties may share sufficient representational structure to benefit from joint learning, while cross-domain properties may not.
2. **Data balance:** Different sample size ratios across tasks determine the severity of negative transfer. Our extreme 65:1 imbalance may have created conditions particularly unfavorable for MTL. Studies with more balanced task sizes may avoid this failure mode.
3. **Material system:** Property relationships may be composition-dependent. Some alloy families (e.g., Ni-based superalloys) may exhibit stronger inter-property correlations due to their specific chemistry and physics, making them more amenable to MTL.

These considerations suggest that MTL success depends critically on property selection and data characteristics, not just the materials domain. Our negative results do not invalidate MTL for materials science broadly; rather, they identify conditions under which caution is warranted. A complete understanding will require systematic studies across diverse material systems and property combinations.

5.6. Limitations and Future Work

5.6.1. Dataset Limitations

Our analysis is limited to one dataset (AI-Hub Korea metal alloys) with three specific properties (resistivity, hardness, amorphous-forming ability). While limiting the study to a single experimental database restricts generalizability, it was a necessary constraint to perform the functional form analysis in Section 3. Large-scale computational databases (e.g., OQMD, Materials Project) were excluded from this study because they lack the specific experimental noise and measurement-availability imbalance (65:1) that characterize real-world experimental archives. Future work should seek to replicate these findings on independent experimental alloy databases (e.g., Citrination) rather than computational proxies.

This scope constrains the generalizability of our conclusions in several important ways:

- **Single dataset:** We cannot claim that our findings represent general principles about MTL in materials science. Different material systems, composition spaces, and property combinations may yield different outcomes.
- **Limited property coverage:** With only three properties spanning different physical domains, we cannot fully test whether within-domain MTL (e.g., hardness + yield strength) would succeed where our cross-domain approach failed. Our preliminary test using derived thermal conductivity (Section 5.4.1) suggests that *independently measured* within-mechanism properties are needed for valid hypothesis testing.

- **Specific imbalance characteristics:** Our extreme 65:1 data imbalance may represent a particularly challenging scenario. Datasets with more balanced task sizes may not experience the same negative transfer.
- **Contradictory recent evidence:** As discussed above, recent studies on different material systems report opposite results (MTL improvements rather than degradation), underscoring that our findings may be dataset- and property-specific.

We explicitly acknowledge that our results should be interpreted as observations on a specific dataset rather than as universal principles. Validation across diverse material systems is essential before general guidelines can be established.

5.6.2. Effectiveness of DIR Mitigation Techniques

Our comprehensive evaluation of DIR techniques (Section 4, Experiment 4) reveals nuanced findings about when each approach is effective:

- **PCGrad** [14]: Highly effective for minority-task protection. The +12.4% improvement on hardness R^2 confirms that gradient conflicts were the primary bottleneck for this task. However, it comes at a cost to majority-task performance (-2.5% on resistivity).
- **GradNorm** [10]: Provides balanced improvements across all tasks through dynamic weight adjustment. Combined with LDS, achieves the best overall performance profile.
- **LDS and Balanced MSE** [17, 18]: Modest improvements for classification (+5.3% F1) but limited benefit for regression tasks when used alone.
- **Negative synergy:** Combining LDS with PCGrad degrades performance compared to PCGrad alone, suggesting these techniques address overlapping mechanisms and may interfere.

These results refine our understanding of task independence. While properties from different physical clusters (electronic vs. mechanical) cannot benefit from shared representations, gradient conflict resolution can still substantially improve minority-task performance by preventing destructive interference during optimization. The functional form mismatch between electronic and mechanical properties remains a structural limitation, but its impact can be mitigated through careful gradient management.

5.6.3. Curriculum Learning

An alternative approach is curriculum learning: first training on the large resistivity dataset to learn general alloy representations, then fine-tuning on smaller datasets. This avoids the interference issues of simultaneous multi-task training while potentially leveraging shared knowledge.

5.6.4. Soft Parameter Sharing

Our soft parameter sharing experiments (Section 4, Experiment 6) reveal that allowing task-specific backbone deviations provides complementary benefits to gradient-based methods:

- **Minority task improvements:** With $\lambda = 0.001$, hardness R^2 improved from 0.735 to 0.764 (+3.9%) and amorphous F1 improved from 0.714 to 0.744 (+4.2%), at a small cost to resistivity (-0.8%).
- **Tail performance:** Soft sharing reduced the maximum hardness prediction error from 3.11 to 1.95 (37% reduction), indicating improved robustness for extreme values.
- **Backbone similarity:** Despite separate backbones, the learned similarity remained high (99.6%), indicating that only subtle task-specific adaptations are needed.

Soft parameter sharing provides a trade-off compared to gradient-based methods: while PCGrad achieves higher overall hardness R^2 (0.855 vs. 0.764), soft sharing may be preferred when tail performance is critical or when gradient manipulation introduces undesirable instabilities.

5.6.5. Feature Distribution Smoothing

FDS (Section 4, Experiment 5) showed no measurable improvement in our setting. This negative result is informative: unlike natural image datasets where FDS was originally developed, alloy composition features are already well-distributed in the compositional simplex. The feature-space imbalance addressed by FDS is distinct from the label-space and task-level imbalance that drives negative transfer in our materials informatics setting. This suggests that DIR techniques should be selected based on the specific nature of the imbalance—feature-space smoothing is ineffective when the imbalance is primarily at the task or label level.

5.6.6. Testing with Independent Measurements

Our derived property experiment (Section 5.4.1) highlights the critical distinction between mechanistic similarity and informational independence. The failure of within-mechanism MTL using derived thermal conductivity demonstrates that shared physics alone is insufficient—auxiliary tasks must provide genuinely independent learning signals. Future work should:

- Collect independently measured within-mechanism property pairs (e.g., resistivity and Seebeck coefficient, both from electronic transport but measured separately)
- Test whether informational independence, rather than physical mechanism, is the true predictor of MTL transfer success
- Develop metrics to quantify the “information overlap” between property datasets prior to MTL training

- Investigate whether the negative result from derived properties generalizes to other physical laws (e.g., Hall-Petch relation for grain size and yield strength)

6. Conclusion

The central finding of this work is that MTL’s value in materials science depends critically on the prediction goal. For high-precision property characterization—where accurate quantitative predictions guide material selection and design—independent single-task models remain superior. For high-throughput screening and discovery—where the goal is to identify promising candidates without missing potential hits—MTL offers meaningful benefits through improved recall, despite reduced precision. This distinction provides practitioners with an actionable framework for deciding when to apply MTL in their materials discovery pipelines.

Our systematic investigation of MTL for metal alloy property prediction, framed around three research questions, yields the following answers:

RQ1 (The Myth): Physical relatedness does *not* guarantee positive transfer. Resistivity and hardness, despite sharing atomic-level dependencies, follow fundamentally different functional forms (Nordheim-type polynomials vs. power-law lattice distortion), creating gradient directions misaligned by 66–75°. Learned task relation graphs confirm this incompatibility with near-zero inter-task weights (~ 0.006). The assumption that “properties sharing physics should share representations” is demonstrably false for this property combination.

RQ2 (The Stress Test): Extreme data imbalance (65:1) compounds functional mismatch to produce severe negative transfer. The majority task dominates the shared backbone, leaving minority tasks to fit their different functional forms using mismatched representations. This manifests as a 16.6% drop in hardness R^2 under standard MTL. However, gradient conflict mitigation techniques—particularly PCGrad (+12.4%) and LDS+GradNorm—can substantially recover performance, confirming that the imbalance is addressable with appropriate optimization strategies.

RQ3 (The Utility): Despite regression degradation, MTL provides practical utility for classification/screening tasks. The 17% improvement in amorphous-forming ability recall means fewer promising candidates are missed during high-throughput screening. The cross-entropy loss scales logarithmically and naturally bounds gradients, making classification robust to the same imbalance that destabilizes regression.

Based on these findings, we offer preliminary guidelines for practitioners working with similar datasets:

- Use independent models when precise property prediction is required for material characterization
- Use MTL for classification/screening tasks where improved recall is valuable for discovery
- Validate MTL assumptions empirically rather than assuming positive transfer from shared physics

- Apply PCGrad when maximizing minority-task performance is the priority
- Use LDS+GradNorm when balanced multi-task performance is desired
- Do not assume combining mitigation techniques yields additive benefits

We hypothesize—but do not validate—that organizing properties by physical mechanism (electronic, mechanical, thermodynamic) may predict MTL compatibility: within-mechanism property pairs may benefit from joint learning, while cross-mechanism combinations require explicit validation. However, our derived property experiment demonstrates that shared physics alone is insufficient—auxiliary tasks must provide informationally independent supervision. Testing this refined hypothesis with independently measured within-mechanism property pairs remains an important direction for future work.

We emphasize that our results are specific to the AI-Hub Korea metal alloy dataset and the three properties studied. Recent contradictory findings in the literature—where MTL improved rather than degraded performance on different material systems—underscore that our observations may not generalize broadly. We present this work as an empirical case study documenting conditions under which MTL can fail, rather than as universal principles. The key contribution is not the specific numerical results, but the demonstration that *when* to use MTL matters as much as *how*—a nuance often overlooked in materials informatics, where “more data” is frequently assumed to be universally beneficial.

Data Availability

The metal alloy property datasets used in this study are available from the AI-Hub Korea platform [30]. Access requires free registration. The datasets include: (1) electrical resistivity measurements (52,388 samples), (2) Vickers hardness measurements (800 samples), and (3) amorphous-forming ability labels (840 samples).

Declaration of Competing Interest

The authors declare that they have no known competing financial interests or personal relationships that could have appeared to influence the work reported in this paper.

References

- [1] J. Schmidt, M. R. Marques, S. Botti, M. A. Marques, Recent advances and applications of machine learning in solid-state materials science, *npj Computational Materials* 5 (1) (2019) 83. doi:10.1038/s41524-019-0221-0.

- [2] K. T. Butler, D. W. Davies, H. Cartwright, O. Isayev, A. Walsh, Machine learning for molecular and materials science, *Nature* 559 (7715) (2018) 547–555. doi:10.1038/s41586-018-0337-2.
- [3] R. Caruana, Multitask learning, *Machine Learning* 28 (1) (1997) 41–75. doi:10.1023/A:1007379606734.
- [4] Y. Zhang, T. Zuo, Z. Tang, M. C. Gao, K. A. Dahmen, P. K. Liaw, Z. P. Lu, Microstructures and properties of high-entropy alloys, *Progress in Materials Science* 61 (2014) 1–93. doi:10.1016/j.pmatsci.2013.10.001.
- [5] T. Xie, J. C. Grossman, Crystal graph convolutional neural networks for an accurate and interpretable prediction of material properties, *Physical Review Letters* 120 (14) (2018) 145301. doi:10.1103/PhysRevLett.120.145301.
- [6] C. Chen, S. P. Ong, Atomsets as a hierarchical transfer learning framework for small and large materials datasets, *npj Computational Materials* 7 (1) (2021) 24. doi:10.1038/s41524-021-00639-w.
- [7] A. Debnath, W. F. Reinhart, Overcoming sparse datasets with multi-task learning as applied to high-entropy alloys, *Machine Learning: Science and Technology* 6 (1) (2025) 015046. doi:10.1088/2632-2153/adb53c.
- [8] Z. Wang, Z. Dai, B. Póczos, J. Carbonell, Characterizing and avoiding negative transfer, in: *Proceedings of the IEEE/CVF Conference on Computer Vision and Pattern Recognition (CVPR)*, IEEE, 2019, pp. 11293–11302.
- [9] T. Standley, A. Zamir, D. Chen, L. Guibas, J. Malik, S. Savarese, Which tasks should be learned together in multi-task learning?, in: *Proceedings of the 37th International Conference on Machine Learning (ICML)*, PMLR, 2020, pp. 9120–9132.
- [10] Z. Chen, V. Badrinarayanan, C.-Y. Lee, A. Rabinovich, Gradnorm: Gradient normalization for adaptive loss balancing in deep multitask networks, in: *Proceedings of the 35th International Conference on Machine Learning (ICML)*, PMLR, 2018, pp. 794–803.
- [11] B. Ramsundar, S. Kearnes, P. Riley, D. Webster, D. Konerding, V. Pande, Massively multitask networks for drug discovery, arXiv preprint arXiv:1502.02072 (2015).
URL <https://arxiv.org/abs/1502.02072>
- [12] M. Wen, S. M. Blau, E. W. C. Spotte-Smith, S. Dwaraknath, K. A. Persson, BonDNet: a graph neural network for the prediction of bond dissociation energies for charged molecules, *Chemical Science* 12 (5) (2021) 1858–1868. doi:10.1039/d0sc05251e.

- [13] M. Crawshaw, Multi-task learning with deep neural networks: A survey, arXiv preprint arXiv:2009.09796 (2020).
- [14] T. Yu, S. Kumar, A. Gupta, S. Levine, K. Hausman, C. Finn, Gradient surgery for multi-task learning, in: *Advances in Neural Information Processing Systems (NeurIPS)*, Vol. 33, Curran Associates, Inc., 2020, pp. 5824–5836.
- [15] A. Kendall, Y. Gal, R. Cipolla, Multi-task learning using uncertainty to weigh losses for scene geometry and semantics, in: *Proceedings of the IEEE/CVF Conference on Computer Vision and Pattern Recognition (CVPR)*, IEEE, 2018, pp. 7482–7491.
- [16] W. Zhang, L. Deng, L. Zhang, D. Wu, A survey on negative transfer, *IEEE/CAA Journal of Automatica Sinica* 10 (2) (2023) 305–329. doi:10.1109/JAS.2022.106004.
- [17] Y. Yang, K. Zha, Y. Chen, H. Wang, D. Katabi, Delving into deep imbalanced regression, in: *Proceedings of the 38th International Conference on Machine Learning (ICML)*, PMLR, 2021, pp. 11842–11851.
- [18] J. Ren, M. Zhang, C. Yu, Z. Liu, Balanced MSE for imbalanced visual regression, in: *Proceedings of the IEEE/CVF Conference on Computer Vision and Pattern Recognition (CVPR)*, IEEE, 2022, pp. 7926–7935.
- [19] A. R. Zamir, A. Sax, W. Shen, L. J. Guibas, J. Malik, S. Savarese, Taskonomy: Disentangling task transfer learning, in: *Proceedings of the IEEE/CVF Conference on Computer Vision and Pattern Recognition (CVPR)*, IEEE, 2018, pp. 3712–3722.
- [20] S. Liu, S. James, A. J. Davison, E. Johns, Auto-Lambda: Disentangling dynamic task relationships, *Transactions on Machine Learning Research* (2022).
URL https://openreview.net/forum?id=r1g2Y_b_C7
- [21] Z. Pei, J. Yin, J. A. Hawk, D. E. Alman, M. C. Gao, Machine-learning informed prediction of high-entropy solid solution formation: Beyond the Hume-Rothery rules, *npj Computational Materials* 6 (1) (2020) 50. doi:10.1038/s41524-020-0308-7.
- [22] S. Kamnis, S. Cadena, P. Sharma, E. Oware Sarpong, N. Dahotre, High-Entropy Alloy property predictions using Transformer-based language model, arXiv preprint arXiv:2411.04861 (2024).
- [23] Z. Rao, P.-Y. Tung, R. Xie, Y. Wei, H. Zhang, A. Ferrari, T. P. C. Klaver, F. Kórmann, P. T. Sukumar, A. K. da Silva, Y. Chen, Z. Li, D. Ponge, J. Neugebauer, O. Gutfleisch, S. Bauer, D. Raabe, Machine learning-enabled high-entropy alloy discovery, *Science* 378 (6615) (2022) 78–85. doi:10.1126/science.abo4940.

- [24] W. Wang, X. Jiang, W. Li, Y. Su, Design of superalloys with multiple properties via multi-task learning, *Acta Materialia* 294 (2025) 121161. doi:10.1016/j.actamat.2025.121161.
- [25] Y. Wang, N. Wagner, J. M. Rondinelli, Symbolic regression in materials science, *MRS Communications* 9 (3) (2019) 793–805. doi:10.1557/mrc.2019.85.
- [26] L. Nordheim, Zur Elektronentheorie der Metalle. I, *Annalen der Physik* 401 (5) (1931) 607–640.
- [27] R. L. Fleischer, Substitutional solution hardening, *Acta Metallurgica* 11 (3) (1963) 203–209. doi:10.1016/0001-6160(63)90213-X.
- [28] R. Labusch, A statistical theory of solid solution hardening, *Physica Status Solidi (b)* 41 (2) (1970) 659–669. doi:10.1002/pssb.19700410221.
- [29] I. Toda-Caraballo, P. E. Rivera-Díaz-del Castillo, Modelling solid solution hardening in high entropy alloys, *Acta Materialia* 85 (2015) 14–23. doi:10.1016/j.actamat.2014.11.010.
- [30] Kairos Lab Inc., Sungkyunkwan University, Yonsei University, Experiment-Based Material Properties Data, <https://aihub.or.kr/aihubdata/data/view.do?dataSetSn=71339>, dataset ID: 71339. Accessed: January 11, 2026 (2022).